

Current bounds on baryogenesis from complex Yukawa couplings of light fermions

Shahaf Aharony Shapira^{1,*}

¹*Department of Particle Physics and Astrophysics,
Weizmann Institute of Science, Rehovot, Israel 7610001*

We calculate the contribution to the baryon asymmetry of the Universe (BAU) from a \mathcal{CP} -violating source of the light quarks (charm, strange, down, up) and the electron, resulting from a dimension-six effective field theory term. We derive relevant bounds from the electric dipole moments of the electron and neutron to estimate the maximal contribution from each single flavor modification. Current bounds show that the charm quark can generate at most $\mathcal{O}(1\%)$ of the BAU, while the lighter quarks and the electron contribute at much lower levels.

Introduction The baryon asymmetry of the Universe (BAU) is defined and measured [1] to be

$$Y_B \equiv \frac{n_B - n_{\bar{B}}}{s} \approx (8.6 \pm 0.1) \cdot 10^{-11} \equiv Y_B^{\text{obs}}, \quad (1)$$

where $n_{(\bar{B})B}$ is the (anti-)baryon number density and s is the entropy density of the Universe. A non-vanishing value can be either the result of initial conditions, or dynamically generated during the early Universe. The former requires fine tuning and is inconsistent with inflation. The latter, which is the more acceptable mechanism to address the asymmetry, is called Baryogenesis.

There are three necessary conditions, known as the Sakharov conditions [2], that are required from any theory in order to explain such an imbalance: Baryon number violation, \mathcal{C} -symmetry and \mathcal{CP} -symmetry violation and interactions out of thermodynamic equilibrium. Although the Standard Model (SM) meets all three criteria, the rate at which it contributes is far too small to account for the observed baryon asymmetry due to two factors: the smooth crossover of the electroweak phase transition and the suppression from the Kobayashi-Maskawa (KM) mechanism of \mathcal{CP} violation. Thus, if the baryon asymmetry was generated via electroweak baryogenesis, the electroweak phase transition had to be strongly first order and a new sources of \mathcal{CP} violation must exist at, or at least not far above, the electroweak scale.

New Physics (NP) beyond the SM is highly motivated by several open questions in Physics (e.g. dark matter, neutrino masses). However, despite the efforts made to discover new particles, none were found up to the TeV scale. It is then plausible, that NP is above the electroweak scale, and thus could be integrated out. This allows us to use Standard Model effective field theory (SMEFT) tools to explore higher order terms, without being model-dependent.

We add a \mathcal{CP} -violating (CPV) phase using a dimension-six (dim-6) coupling of three Higgs fields to the SM charged fermions. The BAU is then proportional to the CPV source, which could be constrained by the

Electric Dipole Moment (EDM) of both the electron and neutron and by the Higgs boson decay. This was previously done for the third generation particles [3] and the muon [4]. Of that list, it was shown that the τ is the only sole-contributor that can provide the entire observed value of the BAU. We generalize this procedure to evaluate the contribution of the light SM quarks (charm, strange, down, up) and the electron and discuss its results here.

This Letter is organized as follows. First, we describe the SMEFT framework, including the complex dim-6 term and the CPV source it generates. We then outline key points in the process of electroweak baryogenesis, which are formulated by the two-step approach via the transport equations followed by the sphaleron process. Next, we present our numerical results for the contribution of a single flavor to the BAU. The contribution is later bounded using the experimental measurements of the electron and neutron EDMs and various Higgs boson decay processes. Finally, we discuss our results and conclusions.

SMEFT framework We examine the implications of adding the following effective dim-6 terms to the SM,

$$\mathcal{L}_{\text{eff Yuk}} = - \left(y_f + \frac{|H|^2}{\Lambda^2} (X_f^R + i\gamma^5 X_f^I) \right) \overline{\psi}_{Lf} \psi_{Rf} H + \text{h.c.}, \quad (2)$$

where y_f is the dimension-four (dim-4) Yukawa coupling, H is the SM Higgs field $H \sim (1, 2)_{+1/2}$, Λ is the NP scale, X is the dim-6 Wilson coefficient and ψ is a SM fermion. In our notation, the lower index, f , denotes the flavor whereas the upper index distinguishes between the real (R) and imaginary (I) coefficients. We find it useful to define

$$T_f^{R,I} \equiv \frac{v^2}{2\Lambda^2} \frac{X_f^{R,I}}{y_f}, \quad (3)$$

where $v = 246$ GeV is the vacuum expectation value (VEV) of the Higgs background field. Accordingly, the mass (m) and effective Yukawa coupling (λ) of each flavor can be defined and explicitly written as

$$\mathcal{L}_{\text{eff Yuk}} \supset -m_f \overline{\psi}_{Lf} \psi_{Rf} - \lambda_f \overline{\psi}_{Lf} \psi_{Rf} h + \text{h.c.}, \quad (4)$$

* shahaf.aharony@weizmann.ac.il

$$m_f = \frac{vy_f}{\sqrt{2}} (1 + T_f^R + iT_f^I), \quad \lambda_f = \frac{y_f}{\sqrt{2}} (1 + 3T_f^R + i3T_f^I). \quad (5)$$

In the mass basis, where $m_f \in \mathbb{R}$, they are given by

$$m'_f = \frac{vy_f}{\sqrt{2}} \sqrt{(1 + T_f^R)^2 + T_f^{I2}},$$

$$\lambda'_f = \frac{y_f}{\sqrt{2}} \frac{(T_f^R + 1)(3T_f^R + 1) + T_f^I(3T_f^I + 2i)}{\sqrt{(1 + T_f^R)^2 + T_f^{I2}}}. \quad (6)$$

Throughout this work we will use the complex parameter κ_f , representing the deviation from the SM in the mass basis,

$$\kappa_f \equiv \frac{\lambda'_f v}{m'_f} = \frac{(T_f^R + 1)(3T_f^R + 1) + T_f^I(3T_f^I + 2i)}{(1 + T_f^R)^2 + T_f^{I2}},$$

$$\kappa_f^I \equiv \text{Im}(\kappa_f) = \frac{2T_f^I}{(1 + T_f^R)^2 + T_f^{I2}}. \quad (7)$$

This notation is convenient since the baryon asymmetry is proportional to the CPV source (S_f) and therefore linear in κ_f^I [3],

$$Y_B \propto S_f \propto \text{Im}(m_f^* m'_f) \propto \kappa_f^I. \quad (8)$$

As we show below, κ_f^I can be constrained by CPV observables, such as the EDMs, and by Higgs-related measurements in colliders.

Electroweak baryogenesis Adding a complex effective Yukawa coupling to one of the fermions of the SM will introduce a CPV source (the explicit form is given in Eqn. (A9)). The source depends on the background Higgs boson field (ϕ_b), which acquires a VEV. Assuming the electroweak phase transition is strongly first order, e.g. assuming ϕ_b is described by the kink solution (Eqn. (A10)), results with a CPV source which peaks mostly inside the non-vanishing VEV bubble. A schematic plot is given in Fig. 1. Namely, the CPV source generates a chiral asymmetry, mainly inside the broken phase. That asymmetry can be transformed into an abundance of baryons via the weak sphaleron, which is a non-perturbative effect of the SM. The rate of the weak sphaleron process is given by $\Gamma_{ws} \sim e^{-(\phi_b)/T} T$, where T is the temperature. Although the rate is exponentially suppressed inside the bubble, it is fast outside the bubble, during the early Universe. Therefore, for baryogenesis to occur at the electroweak phase transition, the chiral asymmetry should have propagated outside the bubble and into the symmetric phase. Finally, as the bubble continues to expand, it eventually captures the resulting baryon asymmetry.

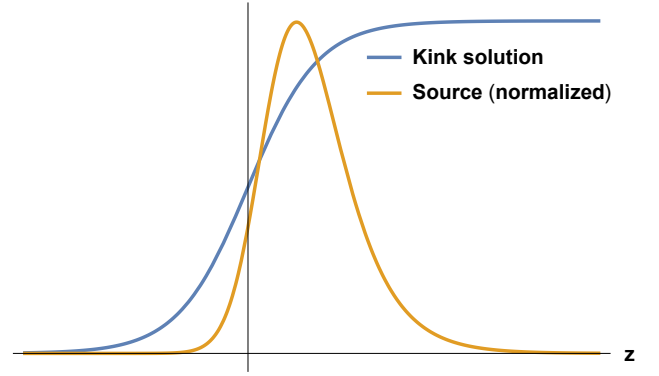


Figure 1: Schematic description of the kink solution and its resulting CPV source along the distance from the bubble wall ($z = 0$). Blue: the kink solution for the background Higgs boson field, as given in Eqn. (A10), orange: the resulting source, normalized.

Two-step approach The dim-6 term described in Eqn. (2) will affect the dynamics of the number densities, which are defined as the difference between the number densities of particles and anti-particles. This effect is the first step of the approach and is described via a set of transport equations. We generalize the set given in [5] to include all the fermions of the SM in addition to the Higgs boson,

$$\begin{aligned} \partial_\mu U_i^\mu &\equiv \partial U_i = -\Gamma_M^{U_i} \mu_M^{U_i} - \Gamma_Y^{U_i} \mu_Y^{U_i} + \Gamma_{ss} \mu_{ss} + S_{U_i}, \\ \partial D_i &= -\Gamma_M^{D_i} \mu_M^{D_i} - \Gamma_Y^{D_i} \mu_Y^{D_i} + \Gamma_{ss} \mu_{ss} + S_{D_i}, \\ \partial Q_i &= -\partial U_i - \partial D_i, \\ \partial E_i &= -\Gamma_M^{E_i} \mu_M^{E_i} - \Gamma_Y^{E_i} \mu_Y^{E_i} + S_{E_i}, \\ \partial L_i &= -\partial E_i, \\ \partial h &= \sum_{i=1}^3 \Gamma_Y^{U_i} \mu_Y^{U_i} - \sum_{i=1}^3 \Gamma_Y^{D_i} \mu_Y^{D_i} - \sum_{i=1}^3 \Gamma_Y^{E_i} \mu_Y^{E_i}, \end{aligned} \quad (9)$$

where U_R, D_R, Q_L are the SM quark fields, E_R, L_L are the SM charged lepton fields (the chirality is implicit hereafter), $\Gamma_{M,Y}$ are the relaxation and Yukawa rates, respectively, and S_f are the CPV sources. The chemical potentials are given by

$$\begin{aligned} \mu_Y^{U_i} &= \frac{U_i}{k_{U_i}} - \frac{Q_i}{k_{Q_i}} - \frac{h}{k_h}, & \mu_M^{U_i} &= \frac{U_i}{k_{U_i}} - \frac{Q_i}{k_{Q_i}}, \\ \mu_Y^{D_i} &= \frac{D_i}{k_{D_i}} - \frac{Q_i}{k_{Q_i}} + \frac{h}{k_h}, & \mu_M^{D_i} &= \frac{D_i}{k_{D_i}} - \frac{Q_i}{k_{Q_i}}, \\ \mu_Y^{E_i} &= \frac{E_i}{k_{E_i}} - \frac{L_i}{k_{L_i}} + \frac{h}{k_h}, & \mu_M^{E_i} &= \frac{E_i}{k_{E_i}} - \frac{L_i}{k_{L_i}}, \\ \mu_{ss} &= \sum_{i=1}^3 \left(\frac{2Q_i}{k_{Q_i}} - \frac{U_i}{k_{U_i}} - \frac{D_i}{k_{D_i}} \right), \end{aligned} \quad (10)$$

where k counts the finite temperature degrees of freedom. All of the benchmark parameters were taken from Ref. [6], and presented in Appendix A. The solution of the transport equations is obtained by reduction of order [6], i.e. N -second order differential equations are written as a set of $2N$ -first order differential equations, and numerical diagonalization. By the second step of the approach the left-handed particles participate in the sphaleron process which generates a baryon asymmetry (Eqn. (B14)).

The two-step procedure is summarized in more detail in Appendix B.

Numerical result Our numerical calculation for the BAU yields

$$Y_B(\kappa_f^I) = -Y_B^{\text{obs}} \cdot (-28\kappa_t^I + 11\kappa_\tau^I + 0.2\kappa_b^I + 0.1\kappa_\mu^I + 0.03\kappa_c^I + 2 \cdot 10^{-4}\kappa_s^I + 3 \cdot 10^{-6}\kappa_e^I + 4 \cdot 10^{-7}\kappa_d^I + 9 \cdot 10^{-8}\kappa_u^I). \quad (11)$$

This result agrees with previous analysis for the third generation particles [3] and the muon [4], but also includes the rest of the charged SM fermions.

We point out that although quarks have (on average) stronger dim-4 Yukawa couplings, which positively impact the CPV source, they also have more washout. It is the result of lower diffusion and higher interaction rates, as well as an additional interaction via the strong sphaleron. This is an important difference between charged leptons and quarks.

Another interesting feature that holds only for the light fermions is that the ratio between contributions of different flavors of either leptons or quarks to the BAU is proportional to the SM Yukawa couplings squared, up to 5%. Thus, for f, f' light flavors of either charged leptons or quarks

$$\frac{Y_B^f}{Y_B^{f'}} \approx \left(\frac{y_f}{y_{f'}}\right)^2 \frac{\kappa_f^I}{\kappa_{f'}^I}. \quad (12)$$

This relation does not hold for the third generation particles, because their interaction rates are orders of magnitude higher.

Finally, the desired κ_f^I that saturates the contribution to the BAU to its observed value could correspond to an unfavorable solution, when demanding the theory to be perturbative. Let us denote the κ_f^I which satisfies $Y_B = Y_B^{\text{obs}}$, according to Eqn. (11), as κ_f^{I*} . By rearranging the definition of κ_f^I (Eqn. (7)), the solution is described by:

$$(T_f^R + 1)^2 + \left(T_f^I - \frac{1}{\kappa_f^{I*}}\right)^2 = \left(\frac{1}{\kappa_f^{I*}}\right)^2, \quad (13)$$

See Fig. 2 for the geometrical interpretation. For large values of κ_f^{I*} , this setting nearly cancels the dim-4 contribution, such that the mass of the fermions is

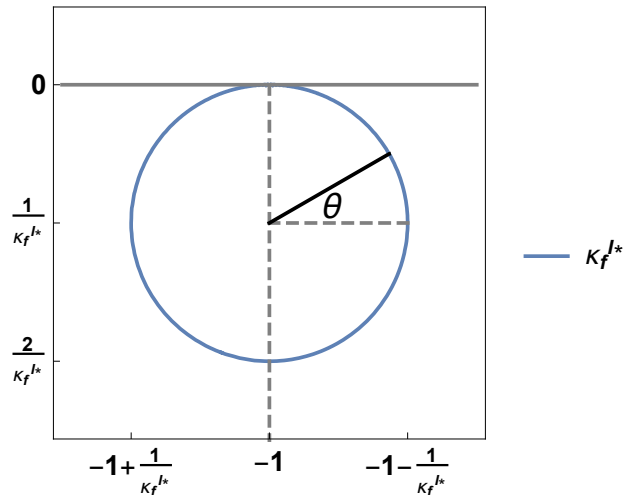


Figure 2: The geometrical description of Eqn. (13) is a circle in (T_f^R, T_f^I) -space centered around $(-1, \frac{1}{\kappa_f^{I*}})$ with radius $\frac{1}{|\kappa_f^{I*}|}$.

effectively generated by the complex part of the dim-6 term, i.e. it requires fine-tuning. Moreover, for some cases, depending on the particle and the position on the circle, it requires $y_f > 4\pi$ which is non-perturbative (See Fig. 3), rendering the analysis moot. We specifically point out the up and down quarks, for which there is no perturbative theory that can account for the observed BAU.

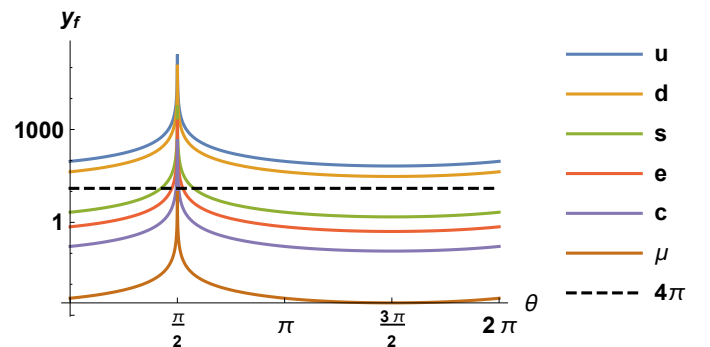


Figure 3: Dim-4 Yukawa coupling y_f as a function of θ , the angle on the circle described in Eqn. (13). The region above the dashed line $y_f = 4\pi$ is non-perturbative and is therefore considered unfavorable. Note that $\theta = \frac{\pi}{2}$, which corresponds to $(-1, 0)$ in (T_f^R, T_f^I) -space, is clearly unphysical and should be excluded for all flavors. The up and down quarks are non-perturbative throughout the entire range, which precludes them as sole-source of the observed BAU.

Bounds The implications of a non-zero κ_f^I are threefold; In addition to the generation of baryon asymmetry, which was discussed above, κ_f^I contributes to the EDMs of the electron and the neutron, and Higgs related measurements. In this Section we use these experimental results to constrain the maximal value of κ_f^I . This will allow us to infer the maximal contribution, from a single flavor modification, to the BAU.

electron-Electric Dipole Moment (eEDM) Bound The upper bound obtained by the ACME collaboration on the eEDM [7] is

$$|d_e^{\max}| = 1.1 \cdot 10^{-29} \text{ e cm at 90\% C.L.} \quad (14)$$

The contribution of the SM fermions, other than the top and the electron, to the eEDM is given by [8, 9]

$$\frac{d_e}{e} \simeq 4N_c Q_f^2 \frac{\alpha}{(4\pi)^3} \frac{m_e m_f^2}{v^2 m_h^2} \left(\ln^2 \left(\frac{m_f^2}{m_h^2} \right) + \frac{\pi^2}{3} \right) \kappa_f^I. \quad (15)$$

The contribution of the top quark to the eEDM is given by [10]

$$\frac{d_e}{e} \simeq 9.4 \cdot 10^{-27} \kappa_t^I \text{ cm}. \quad (16)$$

The contribution of the electron, via two-loop diagrams, to the eEDM is given by [11]

$$\frac{d_e}{e} \simeq 5.1 \cdot 10^{-27} \kappa_e^I \text{ cm}. \quad (17)$$

Neutron-Electric Dipole Moment (nEDM) bound The upper bound obtained by the nEDM collaboration on the nEDM [12] is

$$|d_n^{\max}| = 1.8 \cdot 10^{-26} \text{ e cm at 90\% C.L.} \quad (18)$$

This bound constrains only the κ_f^I of the quarks. The implications of the nEDM bound on $\kappa_{u,d,s}^I$ were calculated in [13]. Here we show the bound, updated to the latest measurement:

$$|\kappa_u^I| \lesssim 0.6, \quad |\kappa_d^I| \lesssim 0.14, \quad |\kappa_s^I| \lesssim 4.5. \quad (19)$$

We also update the bounds on $\kappa_{b,c}^I$ given in [9], assuming $\text{Re}(\kappa_{b,c}) = 0$,

$$|\kappa_b^I| \lesssim 7.4, \quad |\kappa_c^I| \lesssim 13.6. \quad (20)$$

Higgs boson decay Assuming the production rate (σ) of the Higgs boson is unchanged due to the dim-6 operator, the signal strength $\mu_{h \rightarrow f^+ f^-}$ can be written as

$$\begin{aligned} \mu_{i,h \rightarrow f^+ f^-} &\equiv \frac{\sigma_i(pp \rightarrow h) \mathcal{B}(h \rightarrow f^+ f^-)}{\sigma_i^{\text{SM}}(pp \rightarrow h) \mathcal{B}^{\text{SM}}(h \rightarrow f^+ f^-)} \\ &\approx \frac{\mathcal{B}(h \rightarrow f^+ f^-)}{\mathcal{B}^{\text{SM}}(h \rightarrow f^+ f^-)}, \end{aligned} \quad (21)$$

where \mathcal{B} is the branching ratio. It is then straightforward to bound κ_f using the signal strength. For the charged leptons, we translate the upper bound on $\mu_{h \rightarrow \ell\ell}$ to the maximal value of $|\kappa_\ell|$ via

$$\mu_{i,h \rightarrow \ell^+ \ell^-} = \frac{|\kappa_\ell|^2}{1 + (|\kappa_\ell|^2 - 1) \mathcal{B}(h \rightarrow \ell^+ \ell^-)^{\text{SM}}}. \quad (22)$$

For the light quarks, we bound $|\kappa_q|$ via its effect on the total decay width of the Higgs boson. For that we used $\mu_{h \rightarrow b\bar{b}}$ which was measured to be close to unity [14]. When NP interacts with $q = u, c, d, s$, the signal strength of $h \rightarrow b\bar{b}$ is modified as

$$\mu_{h \rightarrow b\bar{b}} = \frac{1}{1 + (|\kappa_q|^2 - 1) \mathcal{B}(h \rightarrow q\bar{q})^{\text{SM}}}. \quad (23)$$

We can then use the experimental bound on $\mu_{h \rightarrow b\bar{b}}$ to constrain the maximal branching fraction as follows:

$$\mathcal{B}(h \rightarrow q\bar{q})^{\max} \lesssim \frac{1}{\mu_{h \rightarrow b\bar{b}}^{\min}} - 1 \approx 0.41, \quad (24)$$

where we used $\mu_{h \rightarrow b\bar{b}}^{\min} \approx 0.71$ at 95% confidence level (C.L.). Assuming the only modification to the SM is the dim-6 term X , we obtain

$$\lambda_q \leq \sqrt{\frac{\mathcal{B}(h \rightarrow q\bar{q})^{\max}}{\mathcal{B}(h \rightarrow b\bar{b})^{\min}}} \frac{y_b}{\sqrt{2}} = \sqrt{\frac{\mathcal{B}(h \rightarrow q\bar{q})^{\max}}{\mu_{h \rightarrow b\bar{b}}^{\min} \mathcal{B}(h \rightarrow b\bar{b})^{\text{SM}}} \frac{y_b}{\sqrt{2}}}. \quad (25)$$

Using the SM prediction $\mathcal{B}(h \rightarrow b\bar{b})^{\text{SM}} = 0.58$, we get, up to $< 1\%$

$$\lambda_q \lesssim \frac{y_b}{\sqrt{2}}. \quad (26)$$

Then, using eqn. (7),

$$|\kappa_q| \lesssim \frac{m_b}{m_q}. \quad (27)$$

Table I: The BAU calculated following the full set of transport equations. Y_B^f is the BAU resulting from S_f . Collider constraints are at $\sim 95\%$ C.L. [3, 14–17]. EDM constraints are at 90% C.L. [7, 12] for all, except for the bottom and charm, for which the nEDM constraints are at 68% C.L. [10].

Source	BAU, Y_B^f	Higgs decay	eEDM	nEDM	maximal % Y_B^{obs}
S_τ	$-9.9 \cdot 10^{-10} \cdot \kappa_\tau^I$	$ \kappa_\tau \lesssim 1.1$	$ \kappa_\tau^I \lesssim 0.3$	-	337%
S_μ	$-1.0 \cdot 10^{-11} \cdot \kappa_\mu^I$	$ \kappa_\mu \lesssim 1.4$	$ \kappa_\mu^I \lesssim 31$	-	17%
S_b	$-2.1 \cdot 10^{-11} \cdot \kappa_b^I$	$ \kappa_b \lesssim 1.7$	$ \kappa_b^I \lesssim 0.2$	$ \kappa_b^I \lesssim 7.4$	5.8%
S_t	$2.4 \cdot 10^{-9} \cdot \kappa_t^I$	$ \kappa_t \lesssim 1.2$	$ \kappa_t^I \lesssim 1.2 \cdot 10^{-3}$	-	3.3%
S_c	$-2.7 \cdot 10^{-12} \cdot \kappa_c^I$	$ \kappa_c \lesssim 3.3$	$ \kappa_c^I \lesssim 0.4$	$ \kappa_c^I \lesssim 13.6$	1.1%
S_s	$-1.6 \cdot 10^{-14} \cdot \kappa_s^I$	$ \kappa_s \lesssim 43$	$ \kappa_s^I \lesssim 109$	$ \kappa_s^I \lesssim 4.5$	0.08%
S_d	$-3.8 \cdot 10^{-17} \cdot \kappa_d^I$	$ \kappa_d \lesssim 890$	$ \kappa_d^I \lesssim 2.3 \cdot 10^4$	$ \kappa_d^I \lesssim 0.14$	$6 \cdot 10^{-6}\%$
S_u	$-8.1 \cdot 10^{-18} \cdot \kappa_u^I$	$ \kappa_u \lesssim 1900$	$ \kappa_u^I \lesssim 2.2 \cdot 10^4$	$ \kappa_u^I \lesssim 0.6$	$6 \cdot 10^{-6}\%$
S_e	$-2.5 \cdot 10^{-16} \cdot \kappa_e^I$	$ \kappa_e \lesssim 266$	$ \kappa_e^I \lesssim 2.2 \cdot 10^{-3}$	-	$6 \cdot 10^{-7}\%$

Results We present our results in Table I. The first prominent result is that no light charged fermion could give the dominant contribution to the BAU. Of all the SM charged fermions only the τ could produce 100% of the observed BAU [3]. The next in importance can be the μ [4], which brings us to consider the relatively negligible effect of the quarks. As mentioned, although the CPV term is proportional to the dim-4 Yukawa coupling squared, which tends to be larger for quarks, they also have more washout than leptons which leads to lower contribution to the BAU. In addition, the bounds are comparable, and thus their maximal percentage is relatively small.

That being said, one could consider two flavor modification, in which case the electron has a special feature. Assuming the interplay of different species does not dramatically change the numerical calculation, the electron could cancel the contribution of another particle to the eEDM, while leaving the contribution to the BAU essentially unchanged. When combined, the interference allows particles that are constrained mostly by the eEDM, such as the top [3], to account for the BAU, e.g. for $\kappa_t^I \approx 0.04$ the top generates Y_B^{obs} , while $\kappa_e^I \approx -0.06$ cancels the top's contribution to the eEDM (See Fig. 4). Because of possible cancellation, it is much harder to exclude such an elusive hypothetical scenario.

Conclusions We consider the CPV source resulting from a dim-6 SMEFT term which couples three Higgs fields to the SM fermions. We generalize the procedure described in Ref. [6] to evaluate the complete set of single flavor modifications from all of the SM charged fermions.

We deduce that although a stronger dim-4 Yukawa coupling enhances the CPV source, quarks have more washout than leptons and are therefore less favorable

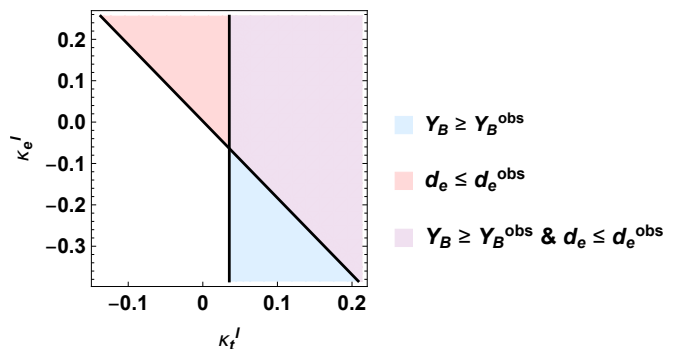


Figure 4: The interplay between the electron and the top could relax the stringent bound on the top, which is from the eEDM measurement. This allows the top to saturate the BAU. Since the next leading bound on both particles is orders of magnitude weaker, such cancellation would be difficult to detect.

candidates to produce the BAU. Moreover, to saturate Y_B^{obs} , some of the particles require non-perturbative dim-4 Yukawa couplings, e.g. the up and down quarks, and are therefore unequivocally ruled out as sole-contributors via this mechanism.

Constrained by the upper bounds of the electron and the neutron EDMs and the Higgs boson decay measurements we evaluate the maximal contribution from each single flavor modification (See Table I). We conclude that the τ is the only candidate able to produce 100% Y_B^{obs} [3]. Other than the μ , which could provide up to 17% Y_B^{obs} [4], the rest of the charged fermions produce negligible contributions (less than 6% Y_B^{obs}). An interplay of different flavors could relax current bounds to allow the observed baryon asymmetry be

accounted for by a CPV Yukawa coupling. Specifically, the interplay of the top and the electron could allow the top to saturate Y_B^{obs} . In addition, off-diagonal couplings should also be considered in a more complete description.

Acknowledgments We are grateful to Yossi Nir and Yehonatan Viernik for helpful discussions.

Appendix A: Benchmark parameters

The input used for this work is the following:

- Coupling constant at nucleation temperature:

$$g_s = 1.23, \quad g = 0.65, \quad g' = 0.36. \quad (\text{A1})$$

- Bubble wall velocity and width:

$$v_w = 0.05, \quad L_w = 0.11 \text{ GeV}^{-1}. \quad (\text{A2})$$

- VEV during nucleation and at 0 temperature:

$$v_N = 152 \text{ GeV}, \quad v_0 = 246 \text{ GeV}. \quad (\text{A3})$$

- The SM fermion masses were taken from [1].

- The diffusion coefficients are calculated in [18]:

$$\begin{aligned} D_{\ell_L} = D_h &= \frac{100}{T}, & D_{\ell_R} &= \frac{380}{T}, \\ D_{q_L} = D_{q_R} &= \frac{6}{T}. \end{aligned} \quad (\text{A4})$$

- The Mass and Yukawa rates are given in Table II. These interaction rates are calculated for $T_I = T_R = 0$.

- The weak sphaleron rate

$$\begin{aligned} \Gamma_{ws} &= 6 \underbrace{\kappa}_{\sim 20} \underbrace{\alpha_w^5}_{\alpha_w = \frac{g^2}{4\pi}} T = 120T \left(\frac{g^2}{4\pi} \right)^5 \\ &\xrightarrow{\text{nucleation}} 120T_N \left(\frac{0.65^2}{4\pi} \right)^5 \approx 4.5 \cdot 10^{-4} \text{ GeV}. \end{aligned} \quad (\text{A5})$$

- The strong sphaleron rate

$$\Gamma_{ss} = 14\alpha_s^4 T \approx 0.26 \text{ GeV}. \quad (\text{A6})$$

- Thermal width:

$$\Gamma_{\text{leptons}} \approx 2 \cdot 10^{-3} T, \quad \Gamma_{\text{quarks}} \approx 0.16 T. \quad (\text{A7})$$

The temperature during nucleation is $T_N = 88 \text{ GeV}$, and for the SM we use $\mathcal{R} = \frac{15}{4}$.

Thermal functions:

- J is given by

$$\begin{aligned} J_e(T) &= \int_0^\infty \frac{k^2 dk}{\omega_L^e \omega_R^e} \text{Im} \left[\frac{n_e(\mathcal{E}_L^e) - n_e(\mathcal{E}_R^{e*})}{(\mathcal{E}_L^e - \mathcal{E}_R^{e*})^2} (\mathcal{E}_L^e \mathcal{E}_R^{e*} - k^2) \right. \\ &\quad \left. + \frac{n_e(\mathcal{E}_L^e) + n_e(\mathcal{E}_R^e)}{(\mathcal{E}_L^e + \mathcal{E}_R^e)^2} (\mathcal{E}_L^e \mathcal{E}_R^e + k^2) \right]. \end{aligned} \quad (\text{A8})$$

- The source is given by

$$\begin{aligned} S_f(z; T) &= \frac{v_w N_c^f}{\pi^2} \text{Im} (m'_f m_f^*) J_f(T) \\ &= \frac{v_w N_c^f y_{\text{SM}}^f}{2\pi^2 v_0^2} J_f(T) \phi_b^3(z) \phi_b'(z) \times \kappa_I^f. \end{aligned} \quad (\text{A9})$$

For the background Higgs boson field we use the kink solution:

$$\phi_b = \frac{v_N}{2} \left(1 + \tanh\left(\frac{z}{L_w}\right) \right). \quad (\text{A10})$$

- The frequencies, energies and Fermi-Dirac distributions are

$$\begin{aligned} \omega_{L,R}^{f_i}(k) &= \sqrt{k^2 + \text{Re}(\delta m_{f_i, L,R}^2(T))}, \\ \mathcal{E}_L^{f_i} &= \omega_{L,R}^{f_i}(k) - i\Gamma_{f_i}, \\ n_f(\mathcal{E}) &= \frac{1}{e^{\frac{\mathcal{E}}{T}} + 1} \end{aligned} \quad (\text{A11})$$

Table II: *Relaxation rates (for the broken phase), and Yukawa rate (for both phases), calculated from [6].*

Particle	Γ_M^B (GeV)	Γ_Y (GeV)
τ	$4.9 \cdot 10^{-3}$	$5.6 \cdot 10^{-4}$
μ	$1.7 \cdot 10^{-5}$	$2.0 \cdot 10^{-6}$
e	$3.9 \cdot 10^{-10}$	$4.4 \cdot 10^{-11}$
t	102	2.6
c	$4.7 \cdot 10^{-3}$	$1.6 \cdot 10^{-4}$
u	$1.4 \cdot 10^{-8}$	$4.7 \cdot 10^{-10}$
b	$5.3 \cdot 10^{-2}$	$1.7 \cdot 10^{-3}$
s	$2.7 \cdot 10^{-5}$	$9.0 \cdot 10^{-7}$
d	$6.5 \cdot 10^{-8}$	$2.1 \cdot 10^{-9}$

- The thermal masses are given by

$$\begin{aligned}
\text{Re}(\delta m_{L_L i}^2(T)) &= \left(\frac{3}{32}g^2 + \frac{1}{32}g'^2 + \frac{1}{16}y_{e_i}^2 \right) T^2 \equiv a_{L_L i}^2 T^2, \\
\text{Re}(\delta m_{e_i R}^2(T)) &= \left(\frac{1}{8}g'^2 + \frac{1}{8}y_{e_i}^2 \right) T^2 \equiv a_{e_i R}^2 T^2, \\
\text{Re}(\delta m_{q_{L_i}}^2(T)) &= \left(\frac{1}{6}g_s^2 + \frac{3}{32}g^2 + \frac{1}{288}g'^2 + \frac{1}{16}y_{u_i}^2 \right. \\
&\quad \left. + \frac{1}{16}y_{d_i}^2 \right) T^2 \equiv a_{q_{L_i}}^2 T^2, \\
\text{Re}(\delta m_{u_i R}^2(T)) &= \left(\frac{1}{6}g_s^2 + \frac{1}{18}g'^2 + \frac{1}{8}y_{u_i}^2 \right) T^2 \equiv a_{u_i R}^2 T^2, \\
\text{Re}(\delta m_{d_i R}^2(T)) &= \left(\frac{1}{6}g_s^2 + \frac{1}{72}g'^2 + \frac{1}{8}y_{d_i}^2 \right) T^2 \equiv a_{d_i R}^2 T^2, \\
\text{Re}(\delta m_h^2(T)) &= \left(\frac{3}{16}g^2 + \frac{1}{16}g'^2 + \frac{1}{12} \sum_{i=e,\mu,\tau} y_{e_i}^2 \right. \\
&\quad \left. + \frac{1}{4} \sum_{i=u,c,t} y_{u_i}^2 + \frac{1}{4} \sum_{i=d,s,b} y_{d_i}^2 \right) T^2 \equiv a_h^2 T^2.
\end{aligned} \tag{A12}$$

- The finite temperature degrees of freedom are given by

$$k_{f_i}(a_{f_i}) = k_0^{f_i} \frac{6}{\pi^2} \int_{a_{f_i}}^{\infty} dx \frac{x e^x}{(e^x \pm 1)^2} \sqrt{x^2 - a_{f_i}^2}. \tag{A13}$$

where k_0^f is the number of degrees of freedom, and + (−) is for fermions (the Higgs boson).

Appendix B: Solving the set of transport equations: the two-step approach

In this appendix we provide further information regarding the analytic techniques we used to calculate the produced baryon asymmetry, similarly to Ref. [6]. We used the two-step approach: First we solve the set of transport equations, as given in Eqn. (9). Then, the baryon asymmetry is obtained by summing over the left-handed number densities and solving an equation which describes the weak sphaleron process.

a. Reduction of dimensions The left hand side of Eqn. (9) can be written as a one dimensional - second order differential equation with respect to the bubble wall dimension denoted z :

$$\begin{aligned}
\partial f &\equiv \partial_\mu f^\mu = \frac{\partial f^0}{\partial t} - \vec{\nabla} \cdot \vec{f} = \underbrace{\frac{\partial z}{\partial t}}_{\equiv v_w} \underbrace{\frac{\partial f^0}{\partial z}}_{f'} + \vec{\nabla} \cdot \left(-D_f \vec{\nabla} f^0 \right) \\
&= v_w f' - D_f \underbrace{\nabla^2 f^0}_{\equiv f''} = v_w f' - D_f f'', \tag{B1}
\end{aligned}$$

where we used Fick's first law and the diffusion approximation.

b. Reduction of order We can solve this set of $N = 16$ - second order differential equations by reduction of order:

$$\begin{aligned}
g_{f_i} &\equiv f'_i, \quad \vec{f} = \left(\vec{U}_R \quad \vec{D}_R \quad \vec{Q}_L \quad \vec{E}_R \quad \vec{L}_L \quad h \right), \quad \vec{\chi} = \left(\vec{f} \quad \vec{g}_f \right)^T. \\
\vec{\chi}' &= \begin{pmatrix} 0 & \mathbb{1}_{N \times N} \\ \hat{\Gamma} & \hat{V} \end{pmatrix} \vec{\chi} + \vec{S} \equiv \hat{K} \vec{\chi} + \vec{S}. \tag{B2}
\end{aligned}$$

We are left with $2N$ -first order differential equations. Then, \hat{K} can be diagonalized numerically using MATLAB.

c. Numerical diagonalization The solution for the symmetric phase is given by

$$\begin{aligned}
\vec{\chi}^S &= \sum_{i=1}^{2N} C_i^S e^{\lambda_i^S z} \vec{u}_i^S \equiv \hat{\Phi}^S(z) \vec{C}^S, \\
\hat{\Phi}_{i,j}^X(z) &= e^{\lambda_{jj}^X z} (\vec{u}_j^X)_i. \tag{B3}
\end{aligned}$$

where C_j 's are constants, λ_j are the eigenvalues, and \vec{u}_j 's are the eigenvectors. We define

$$\hat{\lambda} = \text{diag}(\lambda_i) \quad i = [1 : 2N]. \tag{B4}$$

$$\hat{\phi} = \begin{pmatrix} | & | & & | \\ \vec{u}_1 & \vec{u}_2 & \dots & \vec{u}_{2N} \\ | & | & & | \end{pmatrix} \tag{B5}$$

Accordingly,

$$\hat{\Phi}_{i,j}(z) = \hat{\phi}_{ij} e^{\lambda_{jj} z} = \begin{pmatrix} e^{\lambda_{11} z} \vec{u}_1 & e^{\lambda_{22} z} \vec{u}_2 & \dots & e^{\lambda_{2N 2N} z} \vec{u}_{2N} \end{pmatrix} \tag{B6}$$

The full solution in the broken phase is obtained by variation of parameters to be

$$\vec{\chi}^B = \hat{\Phi}^B(z) \vec{C}^B + \hat{\Phi}^B(z) \int_0^z \left(\hat{\Phi}^B(x) \right)^{-1} \vec{S}(x) dx. \tag{B7}$$

d. Boundary conditions

- The integration constants of the divergent modes in the symmetric phase (which correspond to $\lambda_j^S \leq 0$) are set to zero,

$$C_{0-}^S = 0. \tag{B8}$$

- The positive eigenvalues in the broken phase, C_j^{B+} (which correspond to $\lambda_j^B > 0$), are chosen such that they cancel the divergent part of the full solution at infinity:

$$\vec{C}_+^B = - \int_0^\infty \left(\hat{\Phi}_+^B(x) \right)^{-1} \vec{S}(x) dx. \tag{B9}$$

- We demand continuity at $z = 0$.

– In the symmetric phase we have

$$\vec{\chi}_i^S(z \rightarrow 0^-) = \hat{\phi}_{ij}^S \vec{C}_j^S = \hat{\phi}_{i+}^S \vec{C}_+^S. \quad (\text{B10})$$

– In the broken phase we have

$$\begin{aligned} \vec{\chi}_i^B(z \rightarrow 0^+) &= \hat{\phi}_{ij}^B \vec{C}_j^B = \hat{\phi}_{i(0-)}^B \vec{C}_{0-}^B + \underbrace{\hat{\phi}_{i+}^B \vec{C}_+^B}_{\equiv b_i} \\ &= \hat{\phi}_{i(0-)}^B \vec{C}_{0-}^B + b_i. \end{aligned} \quad (\text{B11})$$

Continuity at $z = 0$ is then

$$\hat{\phi}_{i+}^S \vec{C}_+^S \stackrel{!}{=} \hat{\phi}_{i(0-)}^B \vec{C}_{0-}^B + b_i \longrightarrow \hat{\phi}_{i+}^S \vec{C}_+^S - \hat{\phi}_{i(0-)}^B \vec{C}_{0-}^B = b_i. \quad (\text{B12})$$

We obtain a linear set of equations,

$$\begin{aligned} \hat{\phi}_{SB} &\equiv \begin{pmatrix} | & | \\ \hat{\phi}_{i+}^S & | \\ | & | \\ | & | \end{pmatrix}, \quad \vec{C}_{SB} \equiv \begin{pmatrix} \vec{C}_+^S \\ -\vec{C}_{0-}^B \end{pmatrix}, \\ \hat{\phi}_{SB} \vec{C}_{SB} &\stackrel{!}{=} b_i. \end{aligned} \quad (\text{B13})$$

Solving it sets the rest of the coefficients.

e. The solution The BAU is then given by

$$Y_B = \frac{3\Gamma_{ws}}{2D_q \alpha_+ s} \int_0^{-\infty} e^{-\alpha_- x} n_L(x) dx, \quad (\text{B14})$$

where n_L is the density of left handed particles in the symmetric phase (where the weak sphaleron process is efficient),

$$n_L(z) = \sum_{i=1}^3 (Q_{Li}(z) + L_{Li}(z)), \quad (\text{B15})$$

and

$$\alpha_{\pm} = \frac{1}{2D_q} \left(v_w \pm \sqrt{4D_q \Gamma_{ws} \mathcal{R} + v_w^2} \right) \quad (\text{B16})$$

-
- [1] M. Tanabashi *et al.* [Particle Data Group], Phys. Rev. D **98**, no.3, 030001 (2018)
- [2] A. D. Sakharov, Pisma Zh. Eksp. Teor. Fiz. **5**, 32 (1967) [JETP Lett. **5**, 24 (1967)] [Sov. Phys. Usp. **34**, no. 5, 392 (1991)] [Usp. Fiz. Nauk **161**, no. 5, 61 (1991)].
- [3] E. Fuchs, M. Losada, Y. Nir and Y. Viernik, JHEP **05**, 056 (2020) [arXiv:2003.00099 [hep-ph]].
- [4] E. Fuchs, M. Losada, Y. Nir and Y. Viernik, Phys. Rev. Lett. **124**, no.18, 181801 (2020) [arXiv:1911.08495 [hep-ph]].
- [5] J. De Vries, M. Postma and J. van de Vis, JHEP **04**, 024 (2019) [arXiv:1811.11104 [hep-ph]].
- [6] E. Fuchs, M. Losada, Y. Nir and Y. Viernik, [arXiv:2007.06940 [hep-ph]].
- [7] V. Andreev *et al.* [ACME], Nature **562**, no.7727, 355-360 (2018)
- [8] G. Panico, A. Pomarol and M. Riembau, JHEP **04**, 090 (2019) [arXiv:1810.09413 [hep-ph]].
- [9] J. Brod and E. Stamou, [arXiv:1810.12303 [hep-ph]].
- [10] J. Brod, U. Haisch and J. Zupan, JHEP **11**, 180 (2013) doi:10.1007/JHEP11(2013)180 [arXiv:1310.1385 [hep-ph]].
- [11] W. Altmannshofer, J. Brod and M. Schmaltz, JHEP **05**, 125 (2015) [arXiv:1503.04830 [hep-ph]].
- [12] C. Abel *et al.* [nEDM], Phys. Rev. Lett. **124**, no.8, 081803 (2020) [arXiv:2001.11966 [hep-ex]].
- [13] J. Brod and D. Skodras, JHEP **01**, 233 (2019) [arXiv:1811.05480 [hep-ph]].
- [14] A. M. Sirunyan *et al.* [CMS], Phys. Rev. Lett. **121**, no.12, 121801 (2018) [arXiv:1808.08242 [hep-ex]].
- [15] G. Aad *et al.* [ATLAS], [arXiv:2007.07830 [hep-ex]].
- [16] R. Carlin [CMS], 40th International Conference on High Energy Physics (ICHEP2020), 3 Aug 2020, virtual conference.
- [17] G. Aad *et al.* [ATLAS], Phys. Lett. B **801**, 135148 (2020) [arXiv:1909.10235 [hep-ex]].
- [18] M. Joyce, T. Prokopec and N. Turok, Phys. Rev. D **53**, 2930-2957 (1996) [arXiv:hep-ph/9410281 [hep-ph]].